Advances in Molecular Relaxation and Interaction Processes, 22 (1982) 1–9
Elsevier Scientific Publishing Company, Amsterdam — Printed in The Netherlands

MOLECULAR DYNAMICS SIMULATION OF A LENNARD-JONES TRIATOMIC - TIME AUTO-CORRELATION FUNCTIONS

M.W. EVANS

Chemistry Department, University College of Wales, Aberystwyth, Wales. SY23 1NE (Gt. Britain)

(Received 7 July 1981)

ABSTRACT

The reorientational dynamics of an asymmetric top (a C_{2v} symmetry triatomic) are investigated using molecular dynamics simulation. The angular momentum autocorrelation function $\langle \underline{J}(t).\underline{J}(0)\rangle/\langle J^2(0)\rangle$ is non-exponential with a very long positive tail. The autocorrelation functions $\langle \underline{\ell}_A(t).\underline{\ell}_A(0)\rangle$, $\langle \underline{\ell}_B(t).\underline{\ell}_B(0)\rangle$ and $\langle \underline{\ell}_C(t).\underline{\ell}_C(0)\rangle$ of three unit vectors $\underline{\ell}_A$, $\underline{\ell}_B$ and $\underline{\ell}_C$ fixed in the principle moment of inertia coordinate system are non-exponential for each of the first four Legendre polynomials P_1 to P_4.

INTRODUCTION

In this note we use the method of molecular dynamics simulation to explore the anisotropy of rotational diffusion in a triatomic molecule of C_{2v} symmetry. The relation between the angular momentum auto-correlation function and the orientational a.c.f.'s of an asymmetric top has been the subject of many articles in the recent literature {1} and is generally a difficult problem to tackle analytically. Consequently the technique of molecular dynamics simulation is an ideal method of exploring the basic features of some of the auto-correlation functions of immediate experimental interest {2}. These include the angular momentum and orientational a.c.f.'s. If we denote by $\underline{\ell}_A$, $\underline{\ell}_B$ and $\underline{\ell}_C$ three unit vectors in the asymmetric top along the principal moment of intertia axes, I_A, I_B and I_C then the areas beneath $\langle \underline{\ell}_A(t).\underline{\ell}_A(0)\rangle$, $\langle \underline{\ell}_B(t).\underline{\ell}_B(0)\rangle$ and $\langle \underline{\ell}_C(t).\underline{\ell}_C(0)\rangle$ respectively should produce three correlation times τ_A, τ_B and τ_C related to the three diffusion (and friction) coefficients for rotational diffusion about the three directions A, B and C. These parameters are required for the

0378-4487/82/0000—0000/$02.75

description of, for example, infra-red, far infra-red and dielectric spectra of diffusing asymmetric tops, using theories {3} which depend on an adequate description of the angular momentum autocorrelation function $\langle \underline{J}(t).\underline{J}(0)\rangle$, and the angular velocity autocorrelation function $\langle \underline{\omega}(t).\underline{\omega}(0)\rangle$. Raman and n.m.r. spin-spin correlation times depend on the areas beneath autocorrelation functions such as $\frac{1}{2}\langle(\underline{\ell}_A(t).\underline{\ell}_A(0))^2-1\rangle$ which we denote by P_{2A}, P_{2B} and P_{2C}; P_2 standing for the second Legendre polynomial {4}. Neutron scattering spectra need for their complete description all the N Legendre polynomials, $(N \to \infty)$. We have therefore simulated in this paper P_{3A}, P_{3B} and P_{3C}, together with P_{4A}, P_{4B} and P_{4C}. A thoroughgoing theoretical description would produce adequate estimates of the complete set of Legendre polynomials P_1 to P_N from the angular momentum autocorrelation function $\langle \underline{J}(t).\underline{J}(0)\rangle$.

DESCRIPTION OF THE ALGORITHM

The equations of motion for 108 C_{2v} symmetry triatomics was integrated with a 2 step predictor algorithm developed from the work of Renaud and Singer {5}. The included angle of the triatomic was 56^o, providing moments of inertia (with a bond length of 0.177 nm):

$I_A = 8.09 \times 10^{-46}$ kgm^2

$I_B = 4.77 \times 10^{-46}$ kgm^2

$I_C = 12.85 \times 10^{-46}$ kgm^2

i.e. a markedly asymmetric molecule. Labelling the molecule by ABA the included angle is $\angle$ABA. The mass of the A atom is 35.5 and B is 14 in units of the proton rest mass. The molecules interact through a site-site Lennard-Jones potential with parameters as follows:

A-A; $\varepsilon/k = 173.5$ K; $\sigma = 0.335$ nm

B-B; $\varepsilon/k = 70.5$ K; $\sigma = 0.396$ nm

For the A-B interaction between different molecules we use the combining "rules":

$$\frac{\varepsilon}{k}(A\text{-}B) = \left(\frac{\varepsilon}{k}(A\text{-}A)\frac{\varepsilon}{k}(B\text{-}B)\right)^{\frac{1}{2}}$$

$$\sigma_{A\text{-}B} = \frac{1}{2}(\sigma_{A\text{-}A} + \sigma_{B\text{-}B})$$

The algorithm is constructed in the usual way {6}, using quadrature to integrate the equations of motion of molecules interacting in a pairwise manner with periodic boundary conditions. The first 18 psec of each run consists in melting the assembly of molecules from an initial lattice configuration. The total energy is monitored during each run and when this is constant approximately 600 sets of data for each of the 108 molecules are stored for analysis on 9 track magnetic tapes.

These data are subsequently analysed statistically using a suite of algorithms primarily concerned with computing time autocorrelation functions using a running time averaging technique over the 600 separate configurations of 108 molecules. The sample at equilibrium is tested for isotropy by computing the nine averages $\langle \ell_{AX}^2 \rangle$, $\langle \ell_{AY}^2 \rangle$, $\langle \ell_{AZ}^2 \rangle$, $\langle \ell_{BX}^2 \rangle$, $\langle \ell_{BY}^2 \rangle$, $\langle \ell_{BZ}^2 \rangle$, $\langle \ell_{CX}^2 \rangle$, $\langle \ell_{CY}^2 \rangle$, and $\langle \ell_{CZ}^2 \rangle$, where (X, Y, Z) is the laboratory frame coordinate system. Each of these in an isotropic liquid is ideally 1/3. The simulation results at 293 K, 1bar are recorded in table 1.

RESULTS AND DISCUSSION

The units of the dynamical quantities in the MKS system are related to normalised units used in the algorithm as follows {7}. If we use the symbol to indicate quantities in the algorithm, then

i) $\hat{\underline{r}} = \underline{r}/H$, where $\underline{r}$ is length in metres and H half the box length;

ii) $\hat{\epsilon} = \epsilon/H^2$, where ϵ is the Lennard-Jones energy factor;

iii) $\hat{\underline{F}} = \underline{F}/H$, where $\underline{F}$ is the resultant force on the molecule;

iv) $\hat{\underline{T}} = \underline{T}/H^2$, where $\underline{T}$ is the resultant torque;

v) $\hat{\underline{J}} = \underline{J}/H^2$, where $\underline{J}$ is the resultant angular momentum;

vi) $\hat{\underline{\ell}}_{A,B,C} = \underline{\ell}$, unit vectors in the axes of $I_{A,B,C}$. The vector in the axis bisecting ABA is $\underline{\ell}_A$;

vii) $\hat{\underline{\omega}} = \underline{\omega}$, the angular velocity;

viii) $\hat{I} = I/H^2$, where I is a moment of inertia;

ix) $\hat{\underline{v}} = \underline{v}\,\frac{t}{H}$, where t is the time-step in secs. In the algorithm, $\hat{\underline{v}}$ is in box units per time-step (5×10^{-15} sec).

TABLE 1

Equilibrium Averages of Some Dynamical Quantities

	$\langle \ell_A^2 \rangle$	$\langle \ell_B^2 \rangle$	$\langle \ell_C^2 \rangle$	$\langle \omega^2 \rangle$ /10^{24} s^{-2}	$\langle J^2 \rangle$ /10^{48}(kg $m^2 s^{-2}$)^2	$\langle v^2 \rangle$ /10^5(m s^{-1})^2
X	0.324	0.337	0.340			
Y	0.341	0.323	0.326	5.81	2.81	2.95
Z	0.336	0.330	0.334	5.46	2.71	3.04

In addition to the autocorrelation functions mentioned in the Introduction we have computed the "far infra-red" a.c.f.'s $\langle \underline{\ell}_A(t).\underline{\ell}_A(0) \rangle$, $\langle \underline{\ell}_B(t).\underline{\ell}_B(0) \rangle$ and $\langle \underline{\ell}_C(t).\underline{\ell}_C(0) \rangle$ from the kinematic equations:

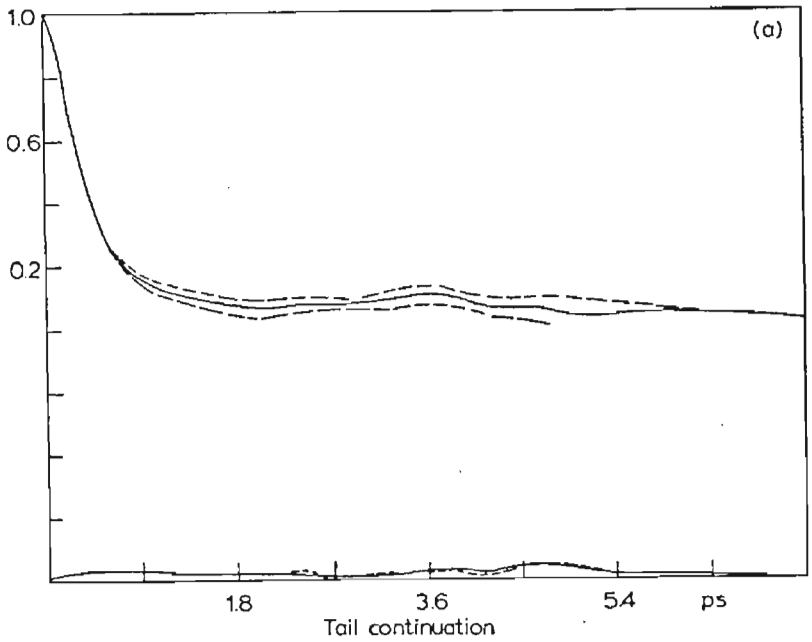

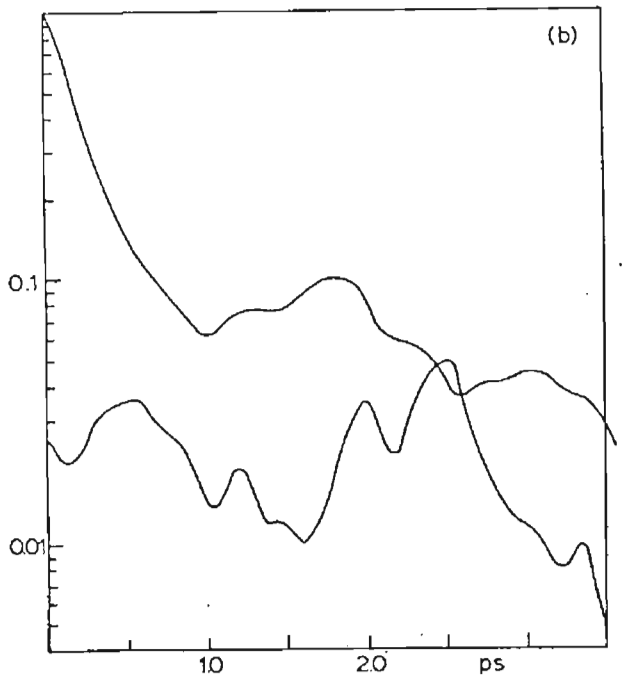

Figure (1)

(a) —— Angular momentum autocorrelation function $\langle \underline{J}(t).\underline{J}(0)\rangle / \langle \underline{J}(0).\underline{J}(0)\rangle$.

– – – (upper) $\langle J_x(t).J_x(0)\rangle / \langle J_x^2(0)\rangle$

----- (lower) $\langle J_y(t).J_y(0)\rangle / \langle J_y^2(0)\rangle$

The time scale in this diagram is twice that of fig.(1b) in order to emphasize the shape of the long time tail.

(b) Angular momentum autocorrelation function $\langle \underline{J}(t).\underline{J}(0)\rangle / \langle \underline{J}(0).\underline{J}(0)\rangle$ on a semi-logarithmic scale, designed to emphasize its non-exponential characteristics.

$\dot{\underline{\ell}}_A = \underline{\omega} \times \underline{\ell}_A$

$\dot{\underline{\ell}}_B = \underline{\omega} \times \underline{\ell}_B$

$\dot{\underline{\ell}}_C = \underline{\omega} \times \underline{\ell}_C$

where $\underline{\omega}$ is the angular velocity. The Fourier transform of $\langle \dot{\underline{\ell}}_A(t) . \dot{\underline{\ell}}_A(0) \rangle$ is the far infra-red power absorption coefficient $\alpha(\omega)$.

In fig.(1) we illustrate the angular momentum a.c.f. $\langle \underline{J}(t) . \underline{J}(0) \rangle / \langle \underline{J}(0) . \underline{J}(0) \rangle$, both on a linear and semi-logarithmic scale. This is very difficult to measure experimentally (spin-rotation N.M.R. relaxation is sometimes useful), but paradoxically is one of the cornerstone functions of the available theory of asymmetric top diffusion {1-3}. We have computed this function to 7 ps using a running time span of 9 ps at thermodynamic equilibrium. The total energy remained acceptably constant with the temperature scaled to 293 K at a molar volume of 6.4×10^{-5} m^3. In fig.(1a) the functions $\langle J_Y(t) . J_Y(0) \rangle / \langle J_Y^2(0) \rangle$ and $\langle J_Z(t) . J_Z(0) \rangle / \langle J_Z^2(0) \rangle$ are shown for comparison. Anisotropy develops in the long positive tail of the three a.c.f.'s after an initial fast decay, covering the first picosecond or so after t = 0. The semi-logarithmic plot exaggerates the role of this tail but it is obvious that the angular momentum a.c.f.'s are not exponential. Memory, as well as inertial, effects are therefore important {4}.

The orientational (Legendre) autocorrelation functions of $\underline{\ell}_A$, $\underline{\ell}_B$ and $\underline{\ell}_C$ decay on the same kind of time scale as the angular momentum a.c.f. This indicates a persistent dynamical memory. If one is using continued fraction algebra to describe the dynamics one therefore needs many approximants to describe the system fully. Numerical techniques developed recently by Grigolini and coworkers {8} enable the numerical solution of the Grigolini/Evans/Ferrario continued fraction {9} using as many as seventy approximants or more in approx. 1 sec of $36^o/37^o$ machine time. Theoretical methods such as these, which use the minimum of adjustable variables (the elements of the Hubbard friction matrix) should aim to reproduce the molecular dynamics indications and, of course, the available spectral data from as many sources as practicable.

In figs.(2a) to (2c) we illustrate the P_N functions (N upt to 4) for the three vectors $\underline{\ell}_A$, $\underline{\ell}_B$ and $\underline{\ell}_C$. These are approximately exponential in their initial decay but this is not maintained in the tails. The correlation times are, as expected, markedly different for each vector. Note that since the liquid is isotropic, the decay of each (X,Y,Z) component of $\underline{\ell}_A$, for example, is virtually identical. The decay of $\underline{\ell}_A$, however, is different from that of $\underline{\ell}_B$ and $\underline{\ell}_C$. If the liquid were anisotropic fro some reason {10} then the decays of all nine possible a.c.f.'s of orientation would be different for each P_N $(N \to \infty)$. This

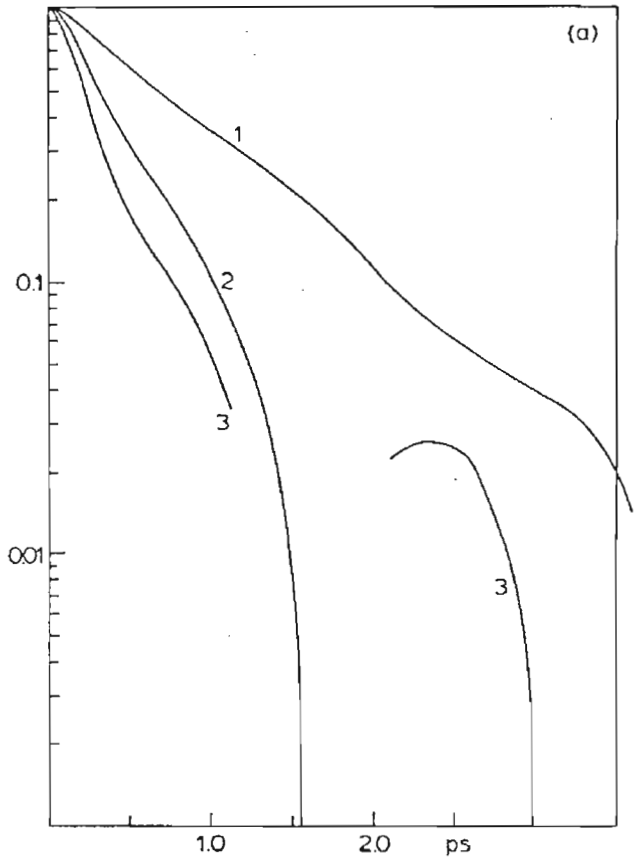
(a)
1
2
3
3
0.1
0.01
1.0
2.0
ps

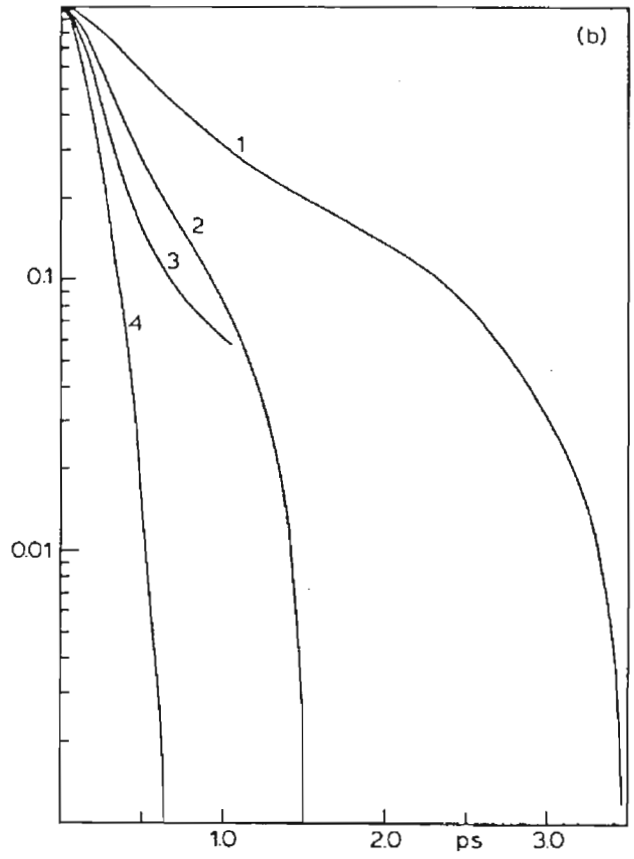
(b)
1
2
3
4
0.1
0.01
1.0
2.0
ps
3.0

is the case in the Kerr effect, for example, or in an aligned nematic. The tails of each simulated P function (twelve in all) overshoot the abscissa to produce negative portions. The molecular dynamics method therefore allows one to calculate in this way the three (diagonal) elements of the asymmetric top friction matrix provided the frame of reference for this matrix is assumed to be the same as the frame of the principal moment of inertia axes. In an anisotropic liquid or asymmetric top of arbitrary symmetry the friction tensor has in general off-diagonal elements in the principal moment of inertia frame. The areas beneath P_{2A}, P_{2B} and P_{2C} may be related to spin-spin N.M.R. times or Raman/Rayleigh correlation times and may be used in N.M.R. theory of diffusing asymmetric tops. The higher Legendre functions may be related to P_1 using Hubbard's equations and the simulation results provide a test for these.

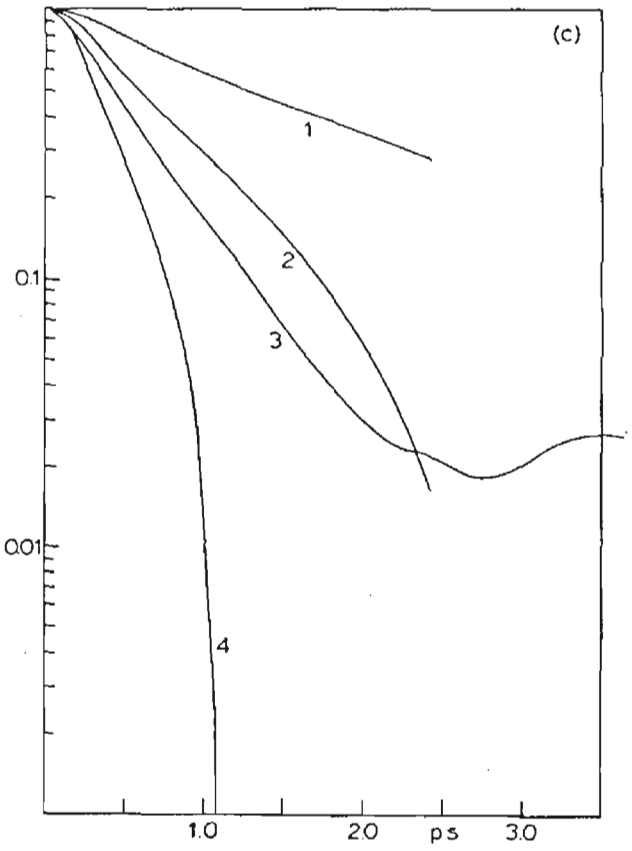

Figure (2)

(a) Decay of P_{1A} to P_{3A} on a semi-logarithmic scale. Note that each Legendre polynomial is non-exponential.

(b) Decay of P_{1B} to P_{4B} on a semi-logarithmic scale.

(c) Decay of P_{1C} to P_{4C} on a semi-logarithmic scale.

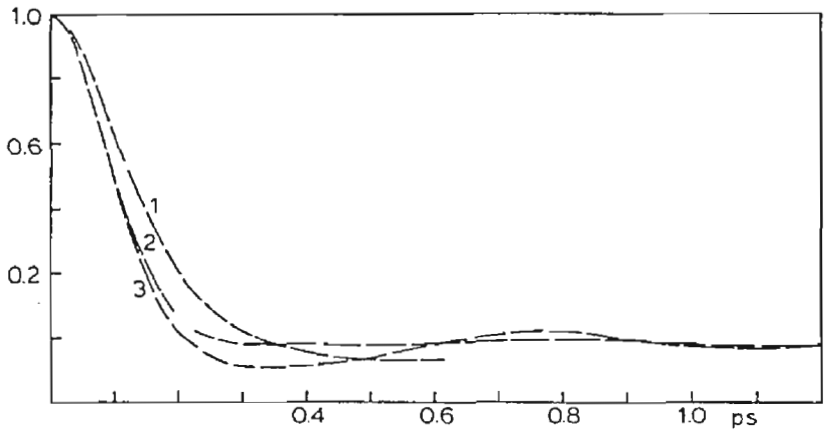

Figure (3)

Rotational velocity autocorrelation functions.

(1) $\langle \underline{\dot{\ell}}_A(t).\underline{\dot{\ell}}_A(0)\rangle$; (2) $\langle \underline{\dot{\ell}}_B(t).\underline{\dot{\ell}}_B(0)\rangle$; (3) $\langle \underline{\dot{\ell}}_C(t).\underline{\dot{\ell}}_C(0)\rangle$.

The analytical theory of neutron-scattering from the asymmetric top is relatively undeveloped, and molecular dynamics simulation is needed here from first principles because of the complexity of the neutron flux interaction. For example, one should avoid the decoupling of rotation from translation.

Finally we remark that the far infra-red functions (fig.(3)) are similar in shape to those observed experimentally, sometimes showing a long negative tail. It is also possible in principle to compute functions such as $\langle \underline{\ddot{\ell}}_A(t).\underline{\ddot{\ell}}_A(0)\rangle$ the Fourier transform (neglecting complications) of $\omega^2\alpha(\omega)$, the far infra-red fourth spectral moment. The sixth moment $\omega^4\alpha(\omega)$ is the F.t. of $\langle \underline{\dddot{\ell}}_A(t).\underline{\dddot{\ell}}_A(0)\rangle$ and so on. Evans {11} has shown recently that $\omega^2\alpha(\omega)$ and $\omega^4\alpha(\omega)$ are observable experimentally with the aid of submillimetre lasers.

We have not dealt with a true molecule in this note but if we increase the angle to 111° and add charges of $0.302|e|$ to CH_2 (atom B) and $-0.151|e|$ to Cl (atom A) we have a good representation of CH_2Cl_2. This asymmetric top will be the subject of future work {12}.

ACKNOWLEDGEMENTS

The S.R.C. is acknowledged for financial support.

REFERENCES

1 For a review, see M.W. Evans, G.J. Evans and A.R. Davies, Adv. Chem. Phys., 44, 255 (1980).

2 M.W. Evans, G.J. Evans, W.T. Coffey and P. Grigolini, "Molecular Dynamics", Wiley/Interscience, N.Y., 1981, in press.

3 W.T. Coffey and B.K.P. Scaife, Proc. R. Irish Acad., 76, 195 (1976); G.W. Ford, J.T. Lewis and J. McConnell, Proc. R. Irish Acad., 76, 117 (1976).

4 B.J. Berne and R. Pecora, "Dynamic Light Scattering with Applications to Chemistry, Physics and Biology", Wiley/ Interscience, N.Y., 1976.

5 Communication of algorithm TRI2.

6 P. Grigolini, M. Ferrario and M.W. Evans, Z. Phys. B., 41, 165 (1981); M.W. Evans, ibid., 39, 75 (1980).

7 D. Fincham, communication.

8 P. Grigolini, M. Marin and M. Giordano, EMLG project communication, in press.

9 P. Grigolini, M.W. Evans and M. Ferrario, Mol. Phys., in press.

10 For a computer simulation of rise and fall transients, see M.W. Evans, J. Chem. Phys. (in press).

11 M.W. Evans, J. Chem. Phys., (in press); Chem. Phys. (in press).

12 Ref. 2, chapter 12; M.W. Evans and J. Yarwood, Adv. Mol. Rel. Int. Proc., in press (EMLG pilot project).